THE ROLE OF ELECTRIC ACTUATION IN THE ELECTRO-CAPILLARY DRIVEN COALESCENCE OF SESSILE DROPLETS: A NUMERICAL STUDY

Datta S.[†]*, Das A. K.[‡] and Das P. K.[†]
*Author for correspondence
[†] Department of Mechanical Engineering, Indian Institute of Technology, Kharagpur, 721302, India
[‡] Department of Mechanical and Industrial Engineering, Indian Institute of Technology Roorkee, 247667, India
E-mail: saikat.mech@gmail.com

ABSTRACT

In the present study, the dynamics of sessile droplet coalescence driven by electro-capillary action (due to external electric field) is investigated numerically. An electro-hydrodynamic model based on finite volume method is used to account the transient electric forces in the two-phase Navier-Stokes equation. The flow field inside the droplet during the initial stages of merging is analyzed thoroughly. The dynamics of electrically driven coalescence is influenced by actuation voltage, droplet volume and the dissimilarity of the coalescing droplet. The internal circulation and kinetic energy produced by the electric stress assists the coalescence. The asymmetry in the velocity and size for dissimilar droplet coalescence produces directional preference in the velocity field. The interplay between surface tension, internal circulation and kinetic energy is analyzed by tracking the dimension of the liquid connection in both parallel and perpendicular direction of the solid surface during coalescence. The outcome of the present study could be utilized in the design of micro-mixers operated by electrostatic actuation.

INTRODUCTION

Over the years, the small scale liquid manipulation inside the Lab-on-a-chip and μ-TAS devices has become very crucial in the field of biomedical and chemical engineering to improve portability and parallelization. Due to low Reynolds number in the small scales, mixing of liquid relies on diffusion. To achieve quick and uniform mixing by diffusion in continuous flow micro mixers split and recombination techniques are success fully used[1-2].In these passive methods the interface area of different fluids are increased by creating multi-lamination layers.

NOMENCLATURE

E	[V/m]	Electric field
f_{elec}	[N]	Volumetric body force due to electric field
n	[-]	Unit normal to the interface
p	[Pa]	Pressure
S	[S/m]	Conductivity
t	[s]	Time
u	[m/s]	Velocity

Special characters

α	[-]	Volume fraction ratio
δ_{sur}	[-]	Direc distribution function
ε	[F/m]	Permittivity
μ_g	[Pa.s]	Density of gas phase
μ_l	[Pa.s]	Density of liquid phase
ρ_c	[C/m^3]	Volumetric charge density
ρ_g	[kg/m^3]	Density of gas phase
ρ_l	[kg/m^3]	Density of liquid phase
ψ	[V]	Electric potential
σ	[N/m]	Surface tension
τ_m	[-]	Maxwell stress tensor

Mixing due to advections is also achieved in continuous flow devices by providing restrictions to the flow [3] or by body forces due to external influences [4]. However, micro manipulation of the liquid in form of a droplet is very convenient to reduce various drawbacks like bubble inclusions and wastage of expensive chemicals etc. The high surface to volume ratio in this case makes the liquid handling extremely difficult. Application of external electric field is a popular way out to this setback [5-6].

The phenomenon of merging by electric actuation is analyzed in both experimental [7-9] as well as numerical [10-11] techniques in previous studies. Cho et al. [7] fabricated a parallel place electrowetting device and checked the viability of droplet merging inside microfluidic devices. The study of Fowler et al.[8] proves that, the rolling of droplet on eletrowetting the surface can achieve fast mixing of large particles. Paik et al. [9] investigated the coalescence of droplets placed between two parallel plates by electrowetting actuation. Their study reveals that the mixing can be enhanced by increasing the number of electrode on which the droplet is oscillating. All these studies are concern to enhance the applicability of electrowetting techniques inside the micro mixtures. From the earlier study [12] of free coalescence it was observed that, the rate of coalescence is increased with external electric field. Thus, questions are still remains open about the role of electrowetting parameters on the hydrodynamics of the initial stages of merging.

Guan and Tong [11] numerically studied the droplet merging in a close type electrowetting system. Their study reveals the effects of different parameters like density, viscosity channel height and surface tension on the coalescence droplet merging. The presence of two walls in an open type increases the internal flow due to shear interaction with the surfaces. But, the internal circulations generated from the release of

interfacial energy get hindered in the presence of walls. For the case of droplet coalescence on an open type electrowetting setup the utilization of the interfacial energy could be higher. However, a few literatures are available to address droplet coalescence on an open type electrowetting platform.

The present study aims to understand the effects of electrowetting parameters on the merging of two sessile droplets situated over open type configuration by numerical simulations. The force due to electric field is estimated by solving a charge conservation and Poisson equation. The electric force in volumetric form is included in the momentum equation as a source term. The interfaces are tracked by volume of fluid (VOF) methods. The next section describes the numerical procedures adopted in the study. The effects of different parameters are discussed at the third section before the salient conclusion at the last.

NUMERICAL METHODOLOGY

Figure 1 illustrates the physical configuration of the present system considered for droplet merging. The droplets are situated on three consecutive electrodes. The size of the middle electrode is equal to the average radius of the droplets and the initial over lap is kept $1/10^{th}$ of the droplet. To trigger coalescence, electric potential is applied on the middle electrodes. Other electrodes are kept ground. Due to the asymmetry in the imposed electric field the free charge and dipoles inside the droplet reorient themselves. As a result charge accumulates at the interfaces. At this scenario, the charge concentration becomes high at the contact line region due to its wedge like shape. Thus, the electromechanical force is large at this region. If the fluids of the droplets are considered to be perfectly conductive, the direction of the electromechanical force will be perpendicular to the surface as schematically shown in Figure 1. The horizontal components of this force try to pull the contact line to move outwards. The asymmetry produced in the menisci creates a pressure gradient inside the droplet. As a result the droplets move toward each other and coalescence occurs.

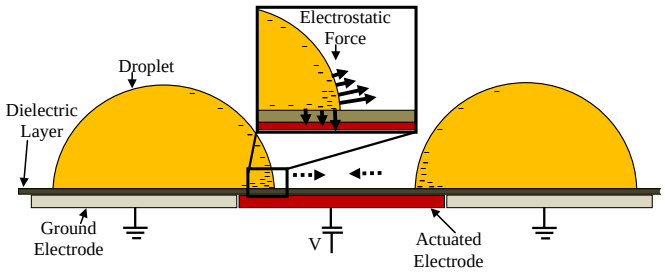

Figure 1 Physical configuration of the present system.

A 3 dimensional electro-hydrodynamic model available in open source Gerris flow solver [13-15] is used to simulate the above phenomena. Poisson equation and a charge conservation equation are solved to obtain the electric field and charge concentration distribution inside the computational domain. The equations can be expressed as:

$$\nabla.(\varepsilon\nabla\psi) = -\rho_c \tag{1}$$

$$\frac{\partial\rho_c}{\partial t} + \nabla.(\rho_c u) = -\frac{S}{\varepsilon}\rho_c \tag{2}$$

Once the electric field is estimated Maxwell's electromagnetic equations are used to obtain the volumetric body force as:

$$\nabla.(\varepsilon\nabla E) = \rho_c \tag{3}$$

$$\nabla\times E = 0 \tag{4}$$

$$f_{elec} = \nabla.\tau_m = \rho_c E - \frac{1}{2}E^2\nabla\varepsilon \tag{5}$$

The electric phenomenon is coupled with the hydrodynamics by incorporation of the volumetric electric force in the incompressible Navier stokes equation as:

$$\nabla.u = 0 \tag{6}$$

$$\rho_m\left(\frac{\partial u}{\partial t} + u.\nabla u\right) = -\nabla p + \nabla.(2\mu\tau_v) + \sigma\lambda\delta_{sur}n + f_{elec} \tag{7}$$

In Gerris a piecewise linear Volume of fluid (VOF) scheme is utilized to track the interface inside the two-phase flow domain. The conservation equation of the volume fraction can be expressed as:

$$\frac{\partial\alpha}{\partial t} + \nabla.(\alpha u) = 0 \tag{8}$$

$$\rho_m = \alpha\rho_l + (1-\alpha)\rho_g \tag{9}$$

$$\mu = \alpha\mu_l + (1-\alpha)\mu_g \tag{10}$$

where, α is volume fraction. ρ and μ are density and viscosity respectively. The subscript l stands for liquid and g stands for gas.

In Gerris the solution of the governing equations are accomplished using a multilevel Poisson solver. The marching in the time domain is carried out by a time-splitting projection method. The staggered-in-time discretization of volume fraction and pressure field results the scheme to be second order accurate in time. Descretization of the advection terms in the momentum equation is done by the second order upwind scheme of Bell et al. [16]. To solve the advection equations in 3D, Gerris uses an Octree adaptive mesh refinement technique [13] for spatial discretization of the computational domain on the basis of predefined criterion. In the octree mesh refinement technique the parent cell is divided into 8 equal sized daughter cells in the immediate higher level. Thus at the n^{th} level, the size of the daughter cells will $1/2^n$ times of the lowest level. In order to capture the generation thin liquid bridge at the onset of coalescence the maximum level of refinement is considered 10 at this region. In all other areas inside the domain the refinement is varied from 4 to 8 based on interface location and vortices.

RESULT AND DISCUSSIONS

In the present study deionised water (S_l=5.6×10^{-6} S/m, ε_l =710×10^{-12} F/m, ρ_l =1000 kg/m^3, μ_l =0.00089 Pa.s) is considered to be the fluid for the droplet. Air (S_g=8.0×10^{-15} S/m, ε_g =8.85×10^{-12} F/m, ρ_g =1.1644 kg/m^3, μ_g =0.0000181 Pa.s) acts as the secondary medium in the numerical simulations. All properties of the liquids are assumed to be homogeneous. Since the droplets are exposed to the electric field for short range of time, the effect of Joule heating is neglected. The equilibrium contact angle of the droplet is 90° with the solid surface. To minimize the influence of the side walls the length of the domain is kept thrice the diameter of the droplet. The width and height of the simulation domain is considered twice the diameter of the droplet. No slip and no penetration boundary condition are applied at the solid walls. The size of the actuated electrode is kept as the average diameter of the droplets. The height and width of the liquid connection formed at the front end of the coalescing droplets (as shown in Figure 2) are used to characterise the phenomenon. In the present study the Reynolds number is varied from =52.77 to 162.56. Thus the phenomenon is considered to fall in the inertial regime. So the inertial time, $t_i = \left(\rho R^3 / \sigma\right)^{\frac{1}{2}}$ could be used to normalize the time [17-118].

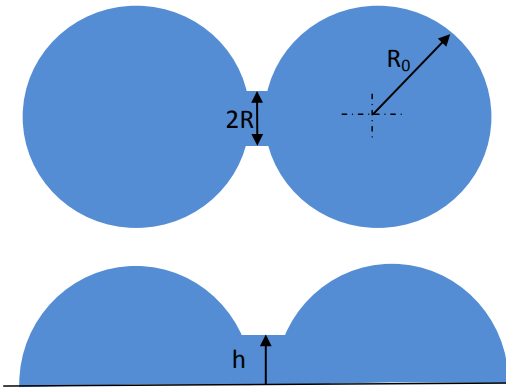

Figure 2 Schematic of the coalesced droplet.

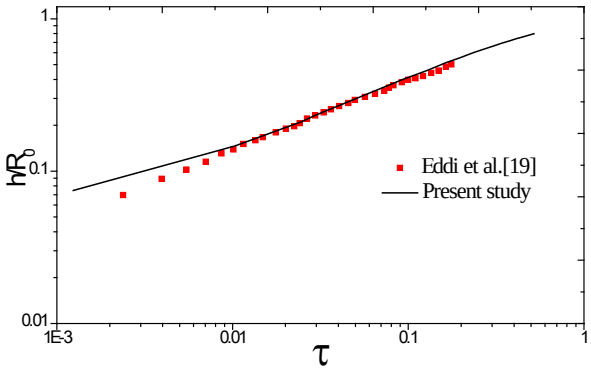

Figure 3 Comparison between the experimental result of Eddi et al.[19] and the present study($\tau = t / t_i$).

In order to check the appropriateness of the present model, the rate of the growth of the liquid bridge height is compared with the experimental result of Eddi et al.[19]. The result of the present simulation closely follows their reported data, where the height of the liquid connection is proportion to the 0.5 exponent of time for the droplets with equilibrium contact angle of 90 °.

In the present study the electric potential is varied from 25 V to 75 V to trigger the coalescence. Figure 4 shows the shape of the interfaces at different time instants during merging actuated with 50 V. Once the potential is applied at the electrode the droplets starts moving towards each other along the actuated electrode (from the initial condition as shown at Figure 1). At the beginning a small liquid bridge is formed at the front as the droplet touches each other. The sharp curvature at the liquid connection increases the local pressure significantly at that region. Thus, there is a fast growth of the liquid bridge. The growth of the liquid bridge draws more fluid into this region. As a result coalescence occurs. After the initial stages of coalescence it takes a shape like a peanut. As the fluid rushes towards the liquid bridge region it gets constrain from the fluid flowing from the opposite side. The resultant flow stretches the droplet in the transverse direction. After a certain time it pushes the liquid back. Once the excess energy is dissipated by viscosity the merged droplet takes a hemispherical shape. At this point it has to be mentioned that, due to the charge concentration at the front end of the droplet there is an initial repulsion. However, the inertia of the actuated droplet is high enough to overcome the repulsive forces.

To understand the hydrodynamics of coalescence further the velocity field during the fusion is studied in detail. Figure 5 depicts the velocity vectors at different time instants in two perpendicular planes for the coalescence of droplets actuated by 50 V. Before discussing the velocity field for coalescence it is worthwhile to mention the same for a single droplet translation actuated by electric field. In our previous report the detail of the velocity vectors inside an electrically actuated droplet is discussed [20]. It was observed that, internal circulations were generated at the edge of the actuated and ground electrode to balance the stress due to potential gradient as a consequence of external electric field; which pumped liquid from the bulk towards the actuated region for drop motion. A similar phenomenon can also be observed in the present case. Here, the vortices (region A) at the junction of the actuated electrode draw liquid towards the merging region (L_2) during coalescence. This aids the growth of liquid bridge further. Figure 5 also illustrates that, the direction of the velocity not remain parallel to the solid surface but changes along the outwards direction at the region (L_1) of the onset of coalescence. This occurs due to the hindrance produced by the inertia of flow from opposite side. The velocity pattern in this region does not change during initial stages of coalescence; however the region (L_1) grows with time gradually affecting more fluid from the bulk and keeping its centre at the initial contact region.

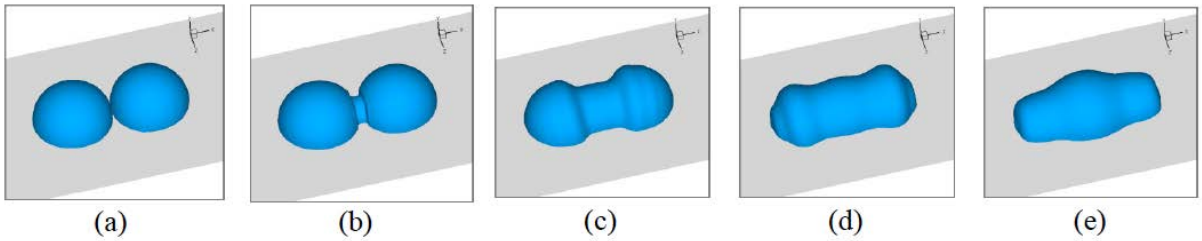

Figure 4 Shape of the interfaces at different time instant during coalescence. Actuation voltage = 50 V; (a)t= 0.00777 s,(b) t=0.00788 s, (c)t=0.00820 s,(d) t=0.00847 s, (e)t=0.00888 s.

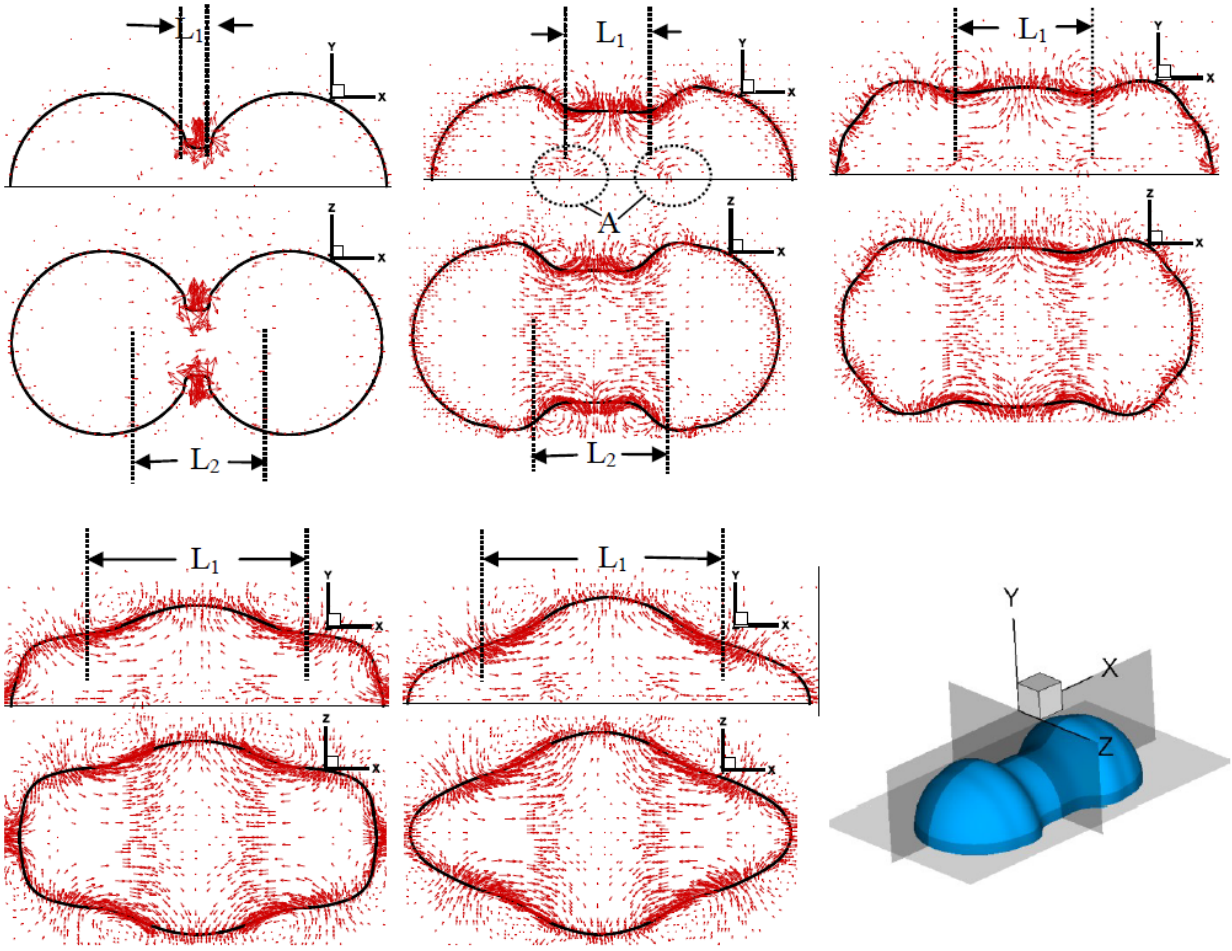

Figure 5 Velocity field inside the droplet during coalescence at different time instant (the times are at increasing order from left to right and top to bottom). Actuation potential and droplet diameter is 50 V and 1 mm respectively.

Effect of actuation potential

The foregoing discussion indicates that, the magnitude of electric potential could have an effect on the coalescence. At larger electric potential the droplets collide with higher kinetic energy. Moreover, the higher potential at the actuated electrode produced a larger electric stress and thus feed more liquid towards the merging region through stronger vortices. To analyze the effect of electric potential quantitatively we track the growth of R and h with time during coalescence. Figure 6 shows the variation of R (scaled with Ro) as a function of non-dimensional time. It can be observed from Figure 6 that, at the onset of merging the liquid bridge expands at a same rate for all electric potentials. This proves the dominance of surface tension force at the initial stages. The effect of electric potential can be observed after the initial stages. After the initial stages, the rate of increase of R is higher for larger actuation voltage. As discussed earlier that, the

experimental studies show the growth rate to be proportional to 0.5 exponent of time for 90° contact angle. Thus, to characterise it in more specific way, the increase of the radius of the droplet with time is at the early stages is shown in log-log plot and compared with $t^{1/2}$ slope (at the inset of Figure 6). The close resemblance proves that, up to a certain time period

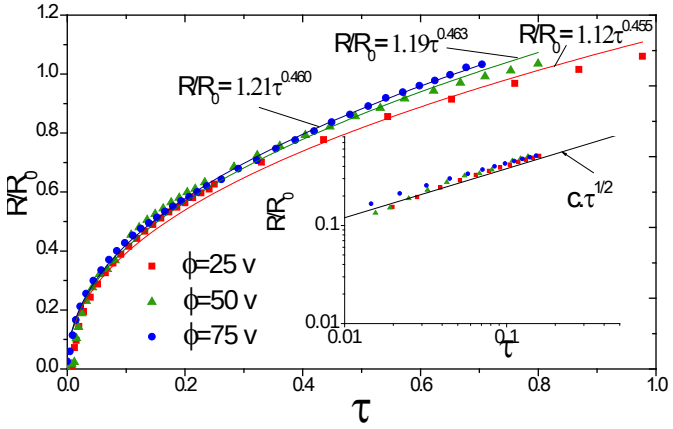

Figure 6 Evolution of the normalized radius of the liquid connection with time during coalescence for different electric potential.

coalescences in the present case is similar to those where droplets are fused without prior velocity. In order to account the whole time span of the growth of the liquid bridge in case of electrostatically propelled coalescence, we estimated the power fit to the simulated result. In the present case the exponent varies from 0.455 to 0.463. The rate of increase of the height of the liquid bridge also illustrates similar behaviour as shown in Figure 7. At the initial stages the increase in the height of the liquid bride also resembles the reported results [19, 21].However, with the electro static actuations the exponents varies from 0.415 to 0.437.

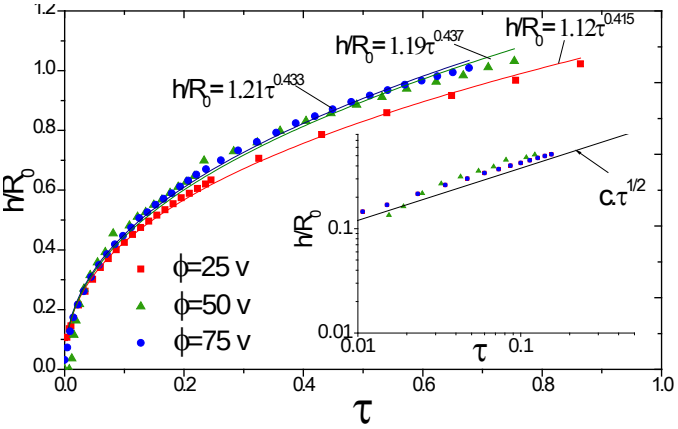

Figure 7 Evolution of the normalized height of the liquid connection with time during coalescence.

Coalescences of different sized droplet

In this section we consider the hydrodynamics of coalescence between different sized droplets. We have simulated the coalescence for dissimilar droplets at 50 V actuation. The diameter of the larger droplet is kept constant at 3 mm. At the same actuation potential smaller droplet moves faster than bigger ones. This is an added asymmetry produced by the electro-wetting actuation in the system along with the dissimilarity in geometry. Figure 8 shows the shape of the interfaces at different time instant during the coalescence between droplets with 1.5 mm and 3 mm diameter. Initially after the formation of the liquid bridge, it grows asymmetrically keeping the wider end towards the larger droplet. The response of fusion reaches earlier at the bulk of the smaller droplet. The fluid from the smaller droplet drained faster towards merged region. As consequence it takes a shape of a protruded finger. Subsequently the protuberance gets absorbed in the merged droplet.

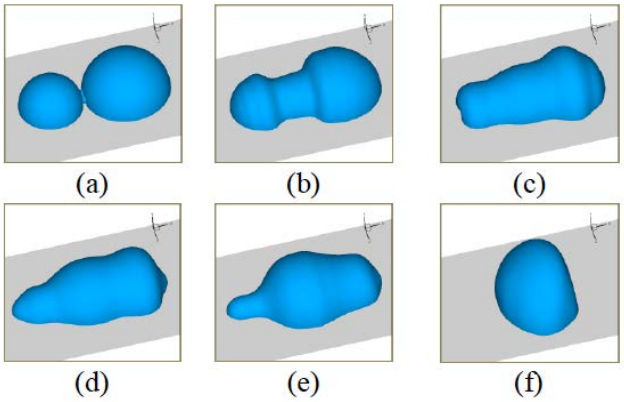

Figure 8 shape of the interface during merging between droplets with 3 mm and 1.5 mm diameter respectively. Actuation voltage = 50 V; (a) t=0.0211 s, (b) t=0.0220 s, (c) t=0.0229 s, (d) t=0.0234 s, (e) t=0.0245 s, (f) t=0.0278 s.

In order to understand the coalescence dynamics of dissimilar droplets further, the velocity field inside the domain is analysed. Figure 9 shows the velocity vectors inside the droplets at different time instant during coalescence between droplets with diameter 1 mm and 3 mm. Initially at the liquid bridge the velocity is outwards similar to the case of droplet with same size. Eventually with the growth of the liquid connection the flow becomes asymmetric. Due to the lesser radius the pressure at the end of smaller droplet size is higher. Moreover, the electrostatic actuation causes the smaller droplet to have higher kinetic energy. Thus the smaller droplet contributes more to the growth of liquid bridge. The liquid from the smaller droplet rapidly drain out towards the bridge region causing a protuberance, as discussed earlier. Due to the presence of surface tension the jutted-out portion is pulled into the bulk fluid. This creates a jet of liquid towards the bulk as shown in Figure 9. Thus, merging of dissimilar droplets is more advantageous in order to achieve better mixing.

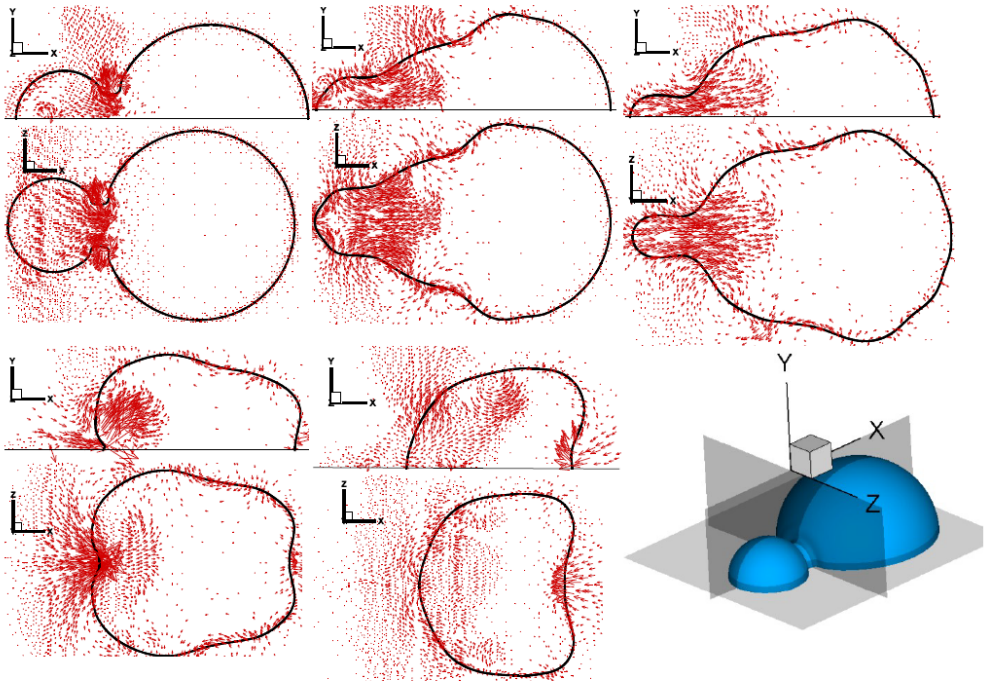

Figure 9 Velocity vector during coalescence between droplets with 3 mm and 1.5 mm diameter

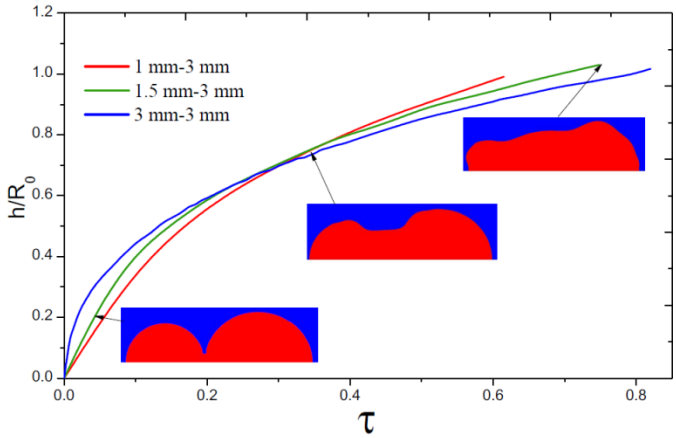

Figure 10 Evolution of the normalized height of the liquid connection with time during coalescence of different sized droplet.

Figure 10 shows the variation of liquid bridge heights for the coalescences of dissimilar droplets. The actuation voltage is considered 50 V for all the cases. In the present case the diameter of the larger droplet is kept fixed at 3 mm and the size of the smaller droplet is varied from 1 mm to 3 mm. As the volume of the larger droplet is fixed, the radius of the smaller droplet is used to normalize the length scale for a comparison. It is evident from the earlier section that, the initial growth of the liquid bridge is dependent on the surface tension. Thus, the higher pressure due to sharper curvature for the case with similar sized droplet makes the bridge growth faster at the early stage. Eventually, the kinetic energy and the pressure of the bulk fluid inside the smaller droplet start dominating. For the same actuation potential the droplet with 1 mm radius have higher kinetic energy. The small radius of curvature also causes the pressure to be larger. As a consequence, the height increases faster after the initial stages in this case. The transverse growth of the liquid bridge also shows identical nature as illustrated in the Figure 11.

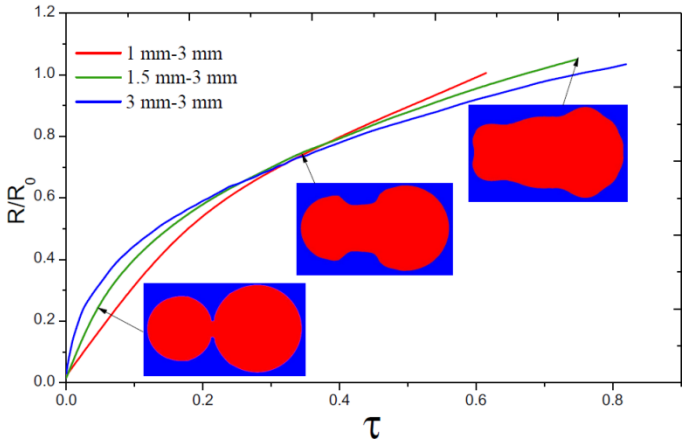

Figure 11 Evolution of the normalized radius of the liquid connection with time during coalescence of different sized droplet.

CONCLUSION

An electro-hydrodynamic scheme is adopted to simulate the droplet coalescence driven by electro static actuation. The velocity field inside the droplet reveals that, for the coalescence of same size droplets the flow pattern inside the merging region

does not change during initial stages of coalescence. In case of dissimilar droplets, the smaller droplet contributes more liquid towards the bridge region due its higher pressure and kinetic energy. The growth rate of the liquid bridge in parallel and perpendicular direction of the solid surface is tracked to analyze the coalescence at different actuation voltages and for dissimilar droplets. The result shows that, the initial growth of the liquid bridge is mainly dominated by surface tension. The effect of electro-wetting actuation is evident after a certain period during bridge growth. The study also reveals that, the initial growth of the liquid bridge is faster for the coalescence between similar droplets than dissimilar ones (due higher curvature of the former). However, the higher pressure and kinetic energy of the smaller droplet drives the growth rate to be higher at the latter stages of liquid bridge expansion.

REFERENCES

[1] Lee, S. W., Kim, D. S., Lee, S. S. and Kwon, T. H.,A split and recombination micromixer fabricated in a PDMS three-dimensional structure", *Journal of Micromechanics and Microengineering*, vol. 16 , 2006, pp:1067–1072

[2] Schönfeld, F., Hessel ,V. and Hofmann, C., An optimised split-and-recombine micro-mixer with uniform 'chaotic' mixing, *Lab on a Chip*, vol. 4, 2004, pp: 65–69.

[3] Kim, D. S., Lee, I. H., Kwon, T. H., Cho, D. W. A Barrier Embedded Kenics Micromixer. *Journal of Micromechanics and Microengineering*, vol. 14, 2004, pp. 1294–1301

[4] Lee, Y. K., Deval, J., Tabeling, P., Ho, C. M. Chaotic Mixing in Electrokinetically and Pressure Driven Micro Flows. *In Micro Electro Mechanical Systems. MEMS 2001. The 14th IEEE International Conference on 2001 Jan 25* (Interlaken, Switzerland),pp. 483–486.

[5] Mugele, F. and Baret, J.C.,Electrowetting: from basics to applications, *Journal of Physics: Condensed Matter*, vol. *17*, 2005,p. R705

[6] Nelson, W.C. and Kim, C.J.C., Droplet actuation by electrowetting-on-dielectric (EWOD): A review. *Journal of Adhesion Science and Technology*, vol. 26, 2012 , pp.1747-1771.

[7] Cho, S.K., Moon, H. and Kim, C.J., Creating, transporting, cutting, and merging liquid droplets by electrowetting-based actuation for digital microfluidic circuits, *Journal of microelectromechanical systems*, vol. *12, 2003* , pp.70-80.

[8] Fowler, J., Moon, H., Chang-Jin, C. K., Enhancement of Mixing by Droplet-Based Microfluidics., *In Proceedings IEEE micro electro mechanical systems*, 2002, pp. 97-100..

[9] Paik, P., Pamula, V.K. and Fair, R.B., Rapid droplet mixers for digital microfluidic systems, *Lab on a Chip*, vol. 3, 2003, pp.253-259.

[10] Aminfar, H. and Mohammadpourfard, M., Droplets merging and stabilization by electrowetting: Lattice Boltzmann study, *Journal of Adhesion Science and Technology*, vol. 26, 2012, pp.1853-1871.

[11] Guan, Y. and Tong, A.Y., Numerical Modeling of Droplet Splitting and Merging in a Parallel-Plate Electrowetting-on-Dielectric (EWOD) Device. *In ASME 2013 4th International Conference on Micro/Nanoscale Heat and Mass Transfer*, December 2013, pp. V001T03A007-V001T03A007

[12] Owe Berg, T.G., Fernish, G.C. and Gaukler, T.A., The mechanism of coalescence of liquid drops. *Journal of the Atmospheric Sciences*, vol. 20, 1963, pp.153-158.

[13] Popinet, S., Gerris: a tree-based adaptive solver for the incompressible Euler equations in complex geometries, *Journal of Computational Physics*, vol. 190, 2003, pp.572-600.

[14] Popinet, S., An accurate adaptive solver for surface-tension-driven interfacial flows, *Journal of Computational Physics*, vol. 228, 2009, pp.5838-5866.

[15] López-Herrera, J.M., Popinet, S. and Herrada, M.A., A charge-conservative approach for simulating electrohydrodynamic two-phase flows using volume-of-fluid, Journal *of Computational Physics*, 230, 2011, pp.1939-1955.

[16] Bell, J.B., Colella, P. and Glaz, H.M., A second-order projection method for the incompressible Navier-Stokes equations, *Journal of Computational Physics*, 85, 1989, pp.257-283.

[17] Wu, M., Cubaud, T. and Ho, C.M., Scaling law in liquid drop coalescence driven by surface tension, *Physics of Fluids*, 16, 2004, pp.L51-L54.

[18] Aarts, D.G., Lekkerkerker, H.N., Guo, H., Wegdam, G.H. and Bonn, D., Hydrodynamics of droplet coalescence, *Physical review letters*, vol. 95, 2005, p.164503.

[19] Eddi, A., Winkels, K.G. and Snoeijer, J.H., Influence of droplet geometry on the coalescence of low viscosity drops, *Physical review letters*, vol. 111, 2013, p.144502.

[20] Datta, S., Das, A.K. and Das, P.K., Uphill movement of sessile droplets by electrostatic actuation, *Langmuir*, 31, 2015, pp.10190-10197.

[21] Sui, Y., Maglio, M., Spelt, P.D., Legendre, D. and Ding, H., Inertial coalescence of droplets on a partially wetting substrate, *Physics of Fluids*, vol. 25, 2013, p.101701.